

Higher-Order estimation of s -th order spectra with flat-top lag-windows

Arthur Berg Dimitris N. Politis

University of California, San Diego

Abstract

Improved performance in higher-order spectral density estimation is achieved using a general class of infinite-order kernels. These estimates are asymptotically less biased but with the same order of variance as compared to the classical estimators with second-order kernels. A simple, data-dependent algorithm for selecting bandwidth is introduced and is shown to be consistent with estimating the optimal bandwidth. Bispectral simulations with several standard models are used to demonstrate the performance of the proposed methodology.

KEYWORDS: Bispectrum, nonparametric estimation, spectral density, time series

1 Introduction

Lag-window estimation of the high-order spectra under various assumptions is known to be consistent and asymptotically normal [1, 2, 10, 11]. However, convergence rates of the estimators depend on the order, or characteristic exponent, of the lag-window used. In general, increasing the order of the lag-window decreases the bias without affecting the order of magnitude of the variance, thus producing an estimator with a faster convergence rate. Although estimators using lag-windows with large orders yield estimates with better mean square error (MSE) rates, they were overlooked and rarely used in practice mainly because of two issues. Firstly, in estimating the second-order spectral density, lag-windows of order larger than two *may* yield negative estimates, despite the fact that the true spectral density is known to be nonnegative. This problem only pertains, if ever, to the second-order spectral density (since higher-order spectra are complex-valued), and is easily remedied by truncating the estimator to zero if it does go negative (thus improving the already optimal convergence rates [13]). Secondly, when a lag-window has order larger than necessary, the rate of convergence is still optimal, but the multiplicative constant will be suboptimal [5]. The second problem is encountered when using a poor choice of large order lag-window like the box-shaped truncated lag-window [13], but there are many other alternatives with descent small-sample performance. Additionally, when the underlying spectral density is sufficiently smooth, this second issue is irrelevant since the lag-window with the largest order

performs best. The next section introduces a family of infinite-order lag-windows for estimating the spectral density and higher-order spectra.

The use of infinite-order lag-windows is particularly adept to the estimation of higher-order spectra. Under the typical scenario of exponential decay of the autocovariance function (refer to part (ii) of Theorem 1 within), the MSE rates for estimating the second-order spectral density using a lag-window of order 2 and an infinite-order lag-window are $N^{-4/5}$ and $(\log N)/N$ respectively. However, when estimating the third-order spectral density, or bispectrum, the MSE rates become $N^{-2/3}$ and $(\log N)/N$ respectively. The disparity grows stronger with yet higher-order spectra.

The problem of choosing the best bandwidth still remains. The optimal bandwidth typically depends on the unknown spectral density leading to a circular problem—estimation of the spectrum requires estimation of the bandwidth which in turn requires estimation of the spectrum. There have been many fixes to this problem; see [8] for a survey of several methods. Section 3 introduces a new simple, data-dependent method of determining the bandwidth which is shown to converge to the asymptotically ideal bandwidth for flat-top lag-windows. An alternative bandwidth selection algorithm is also included that is designed for use with second-order lag-windows. This algorithm uses the plug-in principle for bandwidth selection but with the flat-top estimators as the plug-in pilots.

Particular attention is given to the bispectrum as it is a key tool in several linearity and Gaussianity tests including [6] and [15]. The general bandwidth selection algorithm is refined and expanded for the bispectrum. Bispectral simulations compare two different flat-top lag-windows estimators of the bispectrum with accompanying bandwidth selection algorithm to the lag-window estimator using the order two “optimal” lag-window and plug-in bandwidth selection procedure as described in Rao [16].

We define the flat-top lag-window estimate in Section 2 and derive its higher-order MSE convergence in Theorem 1 under the ideal bandwidth. In Section 3, a bandwidth selection algorithm tailored to the flat-top estimate is introduced and is shown to automatically adapt to the smoothness of the underlying spectral density and converge in probability to the ideal bandwidth. The focus is then shifted to the bispectrum in Section 4 where the most general function invariant under the symmetries of the bivariate cumulant function is constructed. The bandwidth algorithm is specialized for the bispectrum, and a separate bandwidth algorithm for second-order lag-windows is included that is based on the plug-in method with flat-top estimators as pilots. Simulations of the bispectrum in Section 5 exhibit the strength of the flat-top estimators and the bandwidth algorithms.

2 Asymptotic performance of a general flat-top window

Let $\mathbf{x}_1, \mathbf{x}_2, \dots, \mathbf{x}_N$ be a realization of an r -vector valued s^{th} -order stationary (real valued) time series $\mathbf{X}_t = (X_t^{(1)}, \dots, X_t^{(r)})'$ with (unknown) mean $\boldsymbol{\mu} = (\mu^{(1)}, \dots, \mu^{(r)})'$.

Consider the s^{th} -order central moment

$$C''_{a_1, \dots, a_s}(\tau_1, \dots, \tau_s) = \mathbb{E} \left[(X_{t+\tau_1}^{(a_1)} - \mu^{(a_1)}) \dots (X_{t+\tau_s}^{(a_s)} - \mu^{(a_s)}) \right]. \quad (1)$$

where the right-hand side is independent of the choice of $t \in \mathbb{Z}$. Stationarity allows us to write the above moment as function of $s-1$ variables, so we define $C'_{a_1, \dots, a_s}(\tau_1, \dots, \tau_{s-1}) = C''_{a_1, \dots, a_s}(\tau_1, \dots, \tau_{s-1}, 0)$. For notational convenience, the sequence a_1, \dots, a_s will be dropped, so $C'_{a_1, \dots, a_s}(\tau_1, \dots, \tau_{s-1})$ will be denoted simply by $C'(\boldsymbol{\tau})$. Also τ_s will occasionally be used, for convenience, with the understanding that $\tau_s = 0$.

We express the s^{th} -order joint cumulant as

$$C_{a_1, \dots, a_s}(\tau_1, \dots, \tau_{s-1}) = \sum_{(\nu_1, \dots, \nu_p)} (-1)^{p-1} (p-1)! \mu_{\nu_1} \dots \mu_{\nu_p}$$

where the sum is over all partitions (ν_1, \dots, ν_p) of $\{0, \dots, \tau_{s-1}\}$ and $\mu_{\nu_j} = \mathbb{E} \left[\prod_{\tau_i \in \nu_j} X_{\tau_i}^{(a_i)} \right]$; refer to [7] for another expression of the joint cumulant. The (s^{th} -order) spectral density is defined as

$$f(\boldsymbol{\omega}) = \frac{1}{(2\pi)^{s-1}} \sum_{\boldsymbol{\tau} \in \mathbb{Z}^{s-1}} C(\boldsymbol{\tau}) e^{-i\boldsymbol{\tau} \cdot \boldsymbol{\omega}}.$$

We adopt the usual assumption on $C(\boldsymbol{\tau})$ that it be absolutely summable, thus guaranteeing the existence and continuity of the spectral density. A natural estimator of $C(\boldsymbol{\tau})$ is given by

$$\hat{C}(\tau_1, \dots, \tau_{s-1}) = \sum_{(\nu_1, \dots, \nu_p)} (-1)^{p-1} (p-1)! \hat{\mu}_{\nu_1} \dots \hat{\mu}_{\nu_p} \quad (2)$$

where

$$\hat{\mu}_{\nu_j} = \frac{1}{N - \max(\nu_j) + \min(\nu_j)} \sum_{k=-\min(\nu_j)}^{N-\max(\nu_j)} \prod_{t \in \nu_j} x_{t+k}^{(a_j)}$$

It turns out that the second-order and third-order cumulants, those that give rise to the spectrum and bispectrum respectively, are precisely the second-order and third-order central moments 1. Therefore, in these cases, we can greatly simplify $\hat{C}(\boldsymbol{\tau})$ to

$$\hat{C}(\boldsymbol{\tau}) = \frac{1}{N} \sum_{t=1}^{N-\gamma} \prod_{j=1}^s (x_{t-\alpha+\tau_j}^{(a_j)} - \bar{x}^{(a_j)}), \quad (3)$$

where $\alpha = \min(0, \tau_1, \dots, \tau_{k-1})$, $\gamma = \max(0, \tau_1, \dots, \tau_{k-1}) - \alpha$, and $\bar{x}^{(a_\ell)} = \frac{1}{N} \sum_{j=1}^N x_j^{(a_\ell)}$ for $\ell = 1, \dots, s-1$. We extend the domain of \hat{C} to \mathbb{Z}^s by defining $\hat{C}(\boldsymbol{\tau}) = 0$ when then sum in (2) or (3) is empty.

Consider a flat-top lag-window function $\lambda : \mathbb{R}^{s-1} \rightarrow \mathbb{R}$ satisfying the following conditions:

- (i) $\lambda(\boldsymbol{x}) \equiv 1$ for all \boldsymbol{x} satisfying $\|\boldsymbol{x}\| \leq b$, for some positive number b .
- (ii) $|\lambda(\boldsymbol{x})| \leq 1$ for all \boldsymbol{s} .

(iii) For $M \rightarrow \infty$ as $N \rightarrow \infty$, but with $M/N \rightarrow 0$,

$$\lim_{M \rightarrow \infty} \frac{1}{M^{s-1}} \sum_{\|\mathbf{x}\| \leq N} \lambda\left(\frac{\mathbf{x}}{M}\right) < \infty.$$

(iv) $\lambda \in L_2(\mathbb{R}^{s-1})$

The window $\lambda(x)$ is a “flat-top” because of condition (i); namely, it is constant in a neighborhood of the origin. The constant b in (i) is used below in constructing the spectral density estimate.

Technically, just requiring λ just to be bounded could replace criterion (ii), but there is no benefit in allowing the window to have values larger than 1. Finally, criteria (iii) and (iv) are satisfied if, for example, λ has compact support.

Define $\lambda_M(\mathbf{t}) = \lambda(\mathbf{t}/M)$ and consider the smoothed s^{th} -order periodogram

$$\hat{f}(\boldsymbol{\omega}) = \frac{1}{(2\pi)^{s-1}} \sum_{\|\boldsymbol{\tau}\| < N} \lambda_M(\boldsymbol{\tau}) \hat{C}(\boldsymbol{\tau}) e^{-i\boldsymbol{\tau} \cdot \boldsymbol{\omega}}. \quad (4)$$

There is an equivalent expression to this estimator in the frequency domain given by

$$\hat{f}(\boldsymbol{\omega}) = \Lambda_M * I_{a_1, \dots, a_s}(\boldsymbol{\omega}) = \int_{\mathbb{R}^{s-1}} \Lambda_M(\boldsymbol{\omega} - \boldsymbol{\tau}) I_{a_1, \dots, a_s}(\boldsymbol{\tau}) d\boldsymbol{\tau}$$

where Λ_M is the Fourier transform of λ_M and I_{a_1, \dots, a_s} is the $(s-1)^{\text{th}}$ order periodogram; namely,

$$\Lambda_M(\boldsymbol{\tau}) = \int_{\mathbb{R}^{s-1}} \lambda_M(\boldsymbol{\tau}) e^{-i\boldsymbol{\omega} \cdot \boldsymbol{\tau}} d\boldsymbol{\tau}$$

and

$$I_{a_1, \dots, a_s}(\boldsymbol{\omega}) = \frac{1}{(2\pi)^{s-1}} \sum_{\boldsymbol{\tau} \in \mathbb{Z}^{s-1}} \hat{C}(\boldsymbol{\tau}) e^{-i\boldsymbol{\tau} \cdot \boldsymbol{\omega}}$$

However, equation (4) is computationally simpler, and it is this version that will be used throughout the remainder of this article.

The asymptotic bias convergence rate (and thus the overall MSE convergence rate) of the estimator (4) with a flat-top lag-window λ is superior to traditional estimators using second-order lag-windows. The convergence rates of our estimator improve with the decay rate of the cumulant function $C(\boldsymbol{\tau})$ —the faster the decay to zero, the faster the convergence. The following theorem outlines convergence rates under three scenarios: when the decay of $C(\boldsymbol{\tau})$ is polynomial, exponential, and identically zero after some finite time (like an MA(q) process). Throughout, conditions on the time series are assumed so that

$$\text{var}\left(\hat{f}(\boldsymbol{\omega})\right) = O\left(\frac{M^{s-1}}{N}\right). \quad (5)$$

This is a very typical assumption and is satisfied under summability conditions of the cummulants [1] or under certain mixing condition assumptions [11].

Theorem 1. *Let $\{\mathbf{X}_t\}$ be an r -vector valued s^{th} -order stationary time series with unknown mean $\boldsymbol{\mu}$. Let $\hat{f}(\boldsymbol{\omega})$ be the estimator as defined in (4) and assume (5) is satisfied.*

(i) Assume for some $k \geq 1$, $\sum_{\boldsymbol{\tau} \in \mathbb{Z}^{s-1}} \|\boldsymbol{\tau}\|^k |C(\boldsymbol{\tau})| < \infty$ and $M \sim aN^c$ with $c = (2k + s - 1)^{-1}$, then

$$\sup_{\boldsymbol{\omega} \in [-\pi, \pi]^{s-1}} \left| \text{bias} \left\{ \hat{f}(\boldsymbol{\omega}) \right\} \right| = o \left(N^{\frac{-k}{2k+s-1}} \right) \quad (6)$$

and

$$\text{MSE}(\hat{f}(\boldsymbol{\omega})) = O \left(N^{\frac{-2k}{2k+s-1}} \right).$$

(ii) Assume $C(\boldsymbol{\tau})$ decreases geometrically fast, i.e. $|C(\boldsymbol{\tau})| \leq D e^{-d\|\boldsymbol{\tau}\|}$, for some positive constants d and D and $M \sim A \log N$ where $A \geq 1/(2db)$, then

$$\sup_{\boldsymbol{\omega} \in [-\pi, \pi]^{s-1}} \left| \text{bias} \left\{ \hat{f}(\boldsymbol{\omega}) \right\} \right| = O \left(\frac{1}{\sqrt{N}} \right) \quad (7)$$

and

$$\text{MSE} \left(\hat{f}(\boldsymbol{\omega}) \right) = O \left(\frac{\log N}{N} \right). \quad (8)$$

(iii) Assume $C(\boldsymbol{\tau}) = 0$ for $\|\boldsymbol{\tau}\| > q$ and let M be constant such that $bM \geq q$, then

$$\sup_{\boldsymbol{\omega} \in [-\pi, \pi]^{s-1}} \left| \text{bias} \left\{ \hat{f}(\boldsymbol{\omega}) \right\} \right| = O \left(\frac{1}{N} \right)$$

and

$$\text{MSE} \left(\hat{f}(\boldsymbol{\omega}) \right) = O \left(\frac{1}{N} \right)$$

Remark 1. Equations (6), respectively (7), remain true with the assumptions on M replaced with $M^{k+s-1}/N \rightarrow 0$, respectively $e^M M^{s-1}/N \rightarrow 0$.

Remark 2. Depending on the constant A in part (ii), the bias in (7) may be as small as $O((\log N)^{s-1}/N)$.

Remark 3. We do not assume the mean $\boldsymbol{\mu}$ of the time series is known. This adds an extra term of order $O(M^{s-1}/N)$ to the bias; see the proof of Theorem 1 in the appendix for further details.

Remark 4. Traditional estimators using second-order lag-windows have bias convergence rates of order $O(1/M^2)$ regardless of the three scenarios listed in Theorem 1. However when the spectral density is smooth enough, like in the case of an ARMA process (where $C(\boldsymbol{\tau})$ decays exponentially), traditional estimators perform considerably worse. For example, estimation of the bispectrum of an ARMA process has an asymptotic MSE rate of $N^{-2/3}$ in the traditional case, but an asymptotic MSE of $(\log N)/N$ using flat-top lag-windows. The distinction is even more profound in estimating higher-order spectra where the best rate achieved is $N^{-4/(3+s)}$ for traditional estimators and again $(\log N)/N$ using flat-top lag-windows. Even in the worst case of polynomial decay, our proposed estimator still beats, or possibly ties with, traditional estimators in terms of asymptotic MSE rates.

The asymptotic analysis in Theorem 1 relies on having the appropriate bandwidth M based on the various decay rates $C(\boldsymbol{\tau})$. In the next section we propose an algorithm that, for the most part, automatically detects the correct decay rate of $C(\boldsymbol{\tau})$ and supplies the practitioner with an asymptotically consistent estimate of M .

3 A Bandwidth Selection Procedure

For $\boldsymbol{\tau} \in \mathbb{Z}^{s-1}$, consider the normalized cumulant function

$$\rho(\boldsymbol{\tau}) = \frac{C(\boldsymbol{\tau})}{\left(\prod_{i=1}^s C_{a_i}(0)\right)^{1/2}}$$

with natural estimator

$$\hat{\rho}(\boldsymbol{\tau}) = \frac{\hat{C}(\boldsymbol{\tau})}{\left(\prod_{i=1}^s \hat{C}_{a_i}(0)\right)^{1/2}}.$$

Let $B_{x,y}$ ($x, y > 0$) denote the set of indices in \mathbb{Z}^{s-1} contained in the half-open $s - 1$ -dimensional annulus of inner radius x and outer radius y , i.e.

$$B_{x,y} = \{\boldsymbol{\tau} \in \mathbb{Z}^{s-1} : x < \|\boldsymbol{\tau}\| \leq y\}. \quad (9)$$

The following algorithm for estimating the bandwidth of a flat-top estimator is a multivariate extension of an algorithm proposed in [12].

BANDWIDTH SELECTION ALGORITHM

Let $k > 0$ be a fixed constant, and a_N be a nondecreasing sequence of positive integers tending to infinity such that $a_N = o(\log N)$. Let \hat{m} be the smallest number such that

$$|\hat{\rho}(\boldsymbol{\tau})| < k \sqrt{\frac{\log_{10} N}{N}} \quad \text{for all } \boldsymbol{\tau} \in B_{\hat{m}, \hat{m} + a_N} \quad (10)$$

Then let $\hat{M} = \hat{m}/b$ (where b is the “flat-top radius” as defined by condition (i) of a flat-top lag-window).

Remark 5. A norm was not specified in (9) and any norm may be used. The sup norm, for example, may be preferable to the Euclidean norm in practice since the region in (9) becomes rectangular instead of circular.

Remark 6. The positive constant k is irrelevant in the asymptotic theory, but is relevant for finite-sample calculations. In order to determine an appropriate value of c for computation, we consider the following approximation

$$\sqrt{N} (\hat{\rho}(\boldsymbol{\tau}_0) - \rho(\boldsymbol{\tau}_0)) \sim \mathcal{N}(0, \sigma^2). \quad (11)$$

This approximation holds under general assumptions of the time series and for any fixed $\boldsymbol{\tau}_0 \in \mathbb{Z}^{s-1}$. The variance σ^2 does not depend on the choice of $\boldsymbol{\tau}_0$ provided $\boldsymbol{\tau}_0$ is not a “boundary point”; see [2] for more details. Let $\hat{\sigma}$ be the estimate of σ via a resampling scheme like the block bootstrap. A approximate pointwise 95% confidence bound for $\rho(\cdot)$ is given by $\frac{\pm 1.96 \hat{\sigma}}{\sqrt{N}}$. Therefore if we let $a_N = 5$, then $k = 2\hat{\sigma}$ generates an approximate 95% simultaneous confidence bound by Bonferroni’s inequality by noting that $\sqrt{\log_{10} N} \approx 1.5$ for moderately sized N .

The bandwidth selected using the above procedure converges precisely to the ideal bandwidth in each of the three cases of Theorem 1, as is proved in the following theorem under the two natural assumptions in (12) and (13) below¹.

Theorem 2. *Assume conditions strong enough to ensure that for any fixed n ,*

$$\max_{\boldsymbol{\tau} \in B_{0,n}} |\hat{\rho}(\boldsymbol{\sigma} + \boldsymbol{\tau}) - \rho(\boldsymbol{\sigma} + \boldsymbol{\tau})| = O_p \left(\frac{1}{\sqrt{N}} \right) \quad (12)$$

uniformly in $\boldsymbol{\sigma}$, and for any M , that may depend on N , the following holds

$$\max_{\boldsymbol{\tau} \in B_{0,M}} |\hat{\rho}(\boldsymbol{\sigma} + \boldsymbol{\tau}) - \rho(\boldsymbol{\sigma} + \boldsymbol{\tau})| = O_p \left(\sqrt{\frac{\log M}{N}} \right) \quad (13)$$

uniformly in $\boldsymbol{\sigma}$.

(i) *Assume $C(\boldsymbol{\tau}) \sim A \|\boldsymbol{\tau}\|^{-d}$ for some positive constants A and $d \geq 1$. Then*

$$\hat{M} \stackrel{P}{\sim} A_0 \frac{N^{1/2d}}{(\log N)^{1/2d}}$$

where $A_0 = A^{1/d}/(k^{1/d}b)$; here $A \stackrel{P}{\sim} B$ means $A/B \rightarrow 1$ in probability.

(ii) *Assume $C(\boldsymbol{\tau}) \sim A \xi^{\|\boldsymbol{\tau}\|}$ for some positive constant A and $|\xi| < 1$. Then*

$$\hat{M} \stackrel{P}{\sim} A_1 \log N$$

where $A_1 = -1/(b \log |\xi|)$.

(iii) *Suppose $C(\boldsymbol{\tau}) = 0$ when $\|\boldsymbol{\tau}\| > q$, but $C(\boldsymbol{\tau}) \neq 0$ for some $\boldsymbol{\tau}$ with norm q , then $\hat{M} \stackrel{P}{\sim} q/b$.*

4 Bispectrum

Now we will focus on estimating the bispectrum using flat-top lag-windows. The third-order cumulant reduces to the third-order central moment with estimator given by (3). It is easily seen that the third-order central moment, $C(\tau_1, \tau_2)$, satisfies the following symmetry relations:

$$C(\tau_1, \tau_2) = C(\tau_2, \tau_1) = C(-\tau_1, \tau_2 - \tau_1) = C(\tau_1 - \tau_2, -\tau_2) \quad (14)$$

Naturally, we would expect the lag-window function, $\lambda(\tau_1, \tau_2)$, in the estimator (4), to possess the same symmetries. So if a lag-window λ does not a priori have the symmetries as in (14), we can construct a symmetrized version given by

$$\tilde{\lambda} = g(\lambda(x, y), \lambda(y, x), \lambda(-x, y - x), \lambda(y - x, -x), \lambda(x - y, -y), \lambda(-y, x - y)) \quad (15)$$

where g is any symmetric function (of its six variables); for example g could be the geometric or arithmetic mean. It is worth noting that the symmetrized version of λ

¹Under general regularity conditions, (12) holds as does the even stronger assumption of \sqrt{N} asymptotic normality, and (13) holds from general theory of extremes of dependent sequences; refer to [9]

is connected to the theory of group representations of the symmetric group S_3 . As a special case, symmetric lag-windows can be constructed from a one-dimensional lag-window $\lambda(x)$, namely,

$$\tilde{\lambda} = g(\lambda(x), \lambda(y), \lambda(-x), \lambda(y-x), \lambda(x-y), \lambda(-y)) \quad (16)$$

and if $\lambda(x)$ is an even function, then (16) becomes $\tilde{\lambda} = h(\lambda(x), \lambda(y), \lambda(y-x))$ where h is any symmetric function (of its three variables).

Several choices of lag-windows are considered in [17] including the so-called ‘‘optimal window’’, λ_{opt} , which is in some sense optimal among lag-windows of order 2; see Theorem 2 on page 43 of [16]. This lag-window is defined as [14]

$$\lambda_{\text{opt}}(\tau_1, \tau_2) = \frac{8}{\alpha(\tau_1, \tau_2)^2} J_2(\alpha(\tau_1, \tau_2))$$

where J_2 is the second-order Bessel function of the first kind, and

$$\alpha(x, y) = \frac{2\pi}{\sqrt{3}} \sqrt{x^2 - xy + y^2}$$

Although λ_{opt} is optimal among order 2 lag-windows, it is sub-optimal to higher-order lag-windows, such as flat-top lag-windows. Also, since λ_{opt} is not compactly supported, it has the potential of being computationally taxing.

We detail two simple flat-top lag-windows satisfying the symmetries in (14), but the supply of examples is limitless by (15). The first example is a right pyramidal frustum with the hexagonal base $|x| + |y| + |x - y| = 2$. We let $c \in (0, 1)$ be the scaling parameter that dictates when the frustum becomes flat, that is, the flat-top boundary is given by $|x| + |y| + |x - y| = 2c$. The equation of this lag-window is given by

$$\lambda_{\text{rpf}}(\tau_1, \tau_2) = \frac{1}{1-c} \lambda_{\text{rp}}(\tau_1, \tau_2) - \frac{c}{1-c} \lambda_{\text{rp}}\left(\frac{\tau_1}{c}, \frac{\tau_2}{c}\right)$$

where λ_{p} is the equation of the right pyramid with base $|x| + |y| + |x - y| = 2$, i.e.,

$$\lambda_{\text{rp}}(x, y) = \begin{cases} (1 - \max(|x|, |y|))^+, & -1 \leq x, y \leq 0 \text{ or } 0 \leq x, y \leq 1 \\ (1 - \max(|x+y|, |x-y|))^+, & \text{otherwise} \end{cases}$$

The second flat-top lag-window that we propose is the right conical frustum with elliptical base $x^2 - xy + y^2 = 1$. As in the previous example, there is a scaling parameter $c \in (0, 1)$, and the lag-window becomes flat in the ellipse $x^2 - xy + y^2 = c^2$. The equation of this lag-window is given by

$$\lambda_{\text{rcf}}(\tau_1, \tau_2) = \frac{1}{1-c} \lambda_{\text{rc}}(\tau_1, \tau_2) - \frac{c}{1-c} \lambda_{\text{rc}}\left(\frac{\tau_1}{c}, \frac{\tau_2}{c}\right)$$

where λ_{rc} is the equation of the right cone with base $x^2 - xy + y^2 = 1$, i.e.,

$$\lambda_{\text{rc}}(x, y) = (1 - \sqrt{x^2 - xy + y^2})^+$$

Although in both examples the value for b , as defined in property (i) of the flat-top lag-window function, is smaller than the parameter c , the symmetries (14) permit us

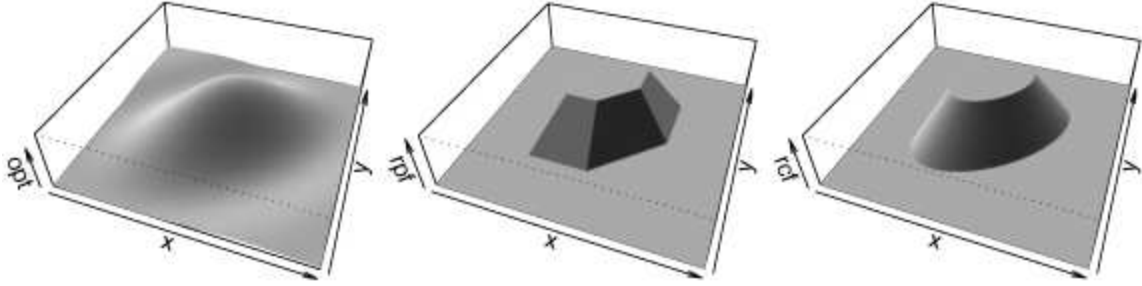


Figure 1: Plots of the three lag-windows, λ_{opt} , λ_{rpf} , and λ_{rpc} (with $c = 1/2$ in the latter two).

to only consider the region $0 \leq y \leq x$ for which a circular arc of radius c does fit. So in the two examples above, we take the value of b to be the parameter c .

The bandwidth selection algorithm can be refined in the context of the bispectrum. The symmetries in (14) allow restriction to the region

$$\{(\tau_1, \tau_2) \in \mathbb{R}^2 \mid 0 \leq \tau_2 \leq \tau_1\} \quad (17)$$

Here is the modified bandwidth selection algorithm for flat-top kernels that is tailored to the bispectrum:

PRACTICAL BANDWIDTH SELECTION ALGORITHM FOR THE BISPECTRUM

Let $\tilde{k} = k_1 > 0$ if $n = 1$, otherwise $\tilde{k} = k_2 > 0$, and let L be a positive integer that is $o(\log N)$. Order the points $\{(\tau_1, \tau_2) \in \mathbb{Z}^2 \mid 0 < \tau_2 < \tau_1\} \cup \{(1, 0)\}$ with the usual lexicographical ordering, so $P_1 = (1, 0)$, $P_2 = (2, 1)$, $P_3 = (3, 1)$, $P_4 = (3, 2)$, and so forth; in general, $P_n = (i, j)$ where $i = \lfloor (\frac{3}{2} + \sqrt{2n - 2}) \rfloor$ and $j = n - \frac{1}{2}(i^2 - 3i) - 2$. Let \hat{m} be the smallest number such that

$$|\hat{\rho}(P_{\hat{m}+\ell})| < \tilde{k} \sqrt{\frac{\log N}{N}} \quad \text{for all } \ell = 1, \dots, L. \quad (18)$$

Then let $\hat{M} = (\text{first coordinate of } P_{\hat{m}}) / b = (\lfloor (\frac{3}{2} + \sqrt{2\hat{m} - 2}) \rfloor) / b$.

Remark 7. Except for the first point, $(1, 0)$, this algorithm does not incorporate boundary points since the asymptotic variance is larger on the boundary; the first point is included as there are no interior points with first coordinate equal to 1. The constant \tilde{k} is adjusted to account for the larger variance in the first point by providing a separate threshold, k_1 , for this point.

Remark 8. As suggested with the general algorithm, a subsampling procedure should be used to determine the appropriate constants k_1 and k_2 . However, one should be careful when choosing a point τ_0 for the approximation (11) since high variances at the origin and on the boundary tend to cause high variances near the origin and near the

boundary in finite-sample scenarios. Therefore an interior point like (6, 3) (as opposed to (2, 1)) should be used in determining k_2 , and a point like (3, 0) (as opposed to (1, 0)) should be used in determining k_1 .

A modified bandwidth selection procedure is now proposed for use with the sub-optimal lag-windows of order 2. In this case, we propose using a bandwidth selection procedure based on the usual “solve-the-equation plug-in” approach [8], but with flat-top estimates of the unknown quantities as the plug-in pilots. This will afford faster convergence rates of the bandwidth as compared estimates based on second-order pilots as well as solve the problem of selecting bandwidths for the pilots.

The optimal bandwidth at each point in the region (17), when using differentiable second order kernels, is derived in [16], and is given by

$$M_\lambda(\omega_1, \omega_2) = \left\{ \frac{\pi N}{\|\lambda\|_{L_2} f(\omega_1) f(\omega_2) f(\omega_1 + \omega_2)} \left(\frac{\partial^2 \lambda(\tau_1, \tau_2)}{\partial \tau_1 \partial \tau_1} \Big|_{\tau_1 = \tau_2 = 0} \right)^2 \times \right. \\ \left. \times \left| \left(\frac{\partial^2}{\partial \omega_1^2} - \frac{\partial^2}{\partial \omega_1 \partial \omega_2} + \frac{\partial^2}{\partial \omega_2^2} \right) f(\omega_1, \omega_2) \right|^2 \right\}^{\frac{1}{6}} \quad (19)$$

Estimates of the spectral density using flat-top lag-windows is discussed above, and estimating the partial derivatives of the bispectrum follow similarly. For instance, the three second order partial derivatives needed in (19) can be estimated by

$$\widehat{f_{\omega_i, \omega_j}}(\omega_1, \omega_2) = \frac{\partial^2}{\partial \omega_i \partial \omega_j} \hat{f}(\omega_1, \omega_2) \\ = \frac{1}{(2\pi)^2} \sum_{\tau_1 = -N}^N \sum_{\tau_2 = -N}^N \tau_i \tau_j \lambda_M(\tau_1, \tau_2) \widehat{C}(\tau_1, \tau_2) e^{-i\tau \cdot \omega} \quad i, j = 1, 2. \quad (20)$$

By mimicking the proof of Theorem 1, the estimator in (20) has the same asymptotic performance as the estimator $\hat{f}(\omega)$ in Theorem 1 but under a slightly stronger assumption for part (i) that $\sum_{\tau \in \mathbb{Z}^2} \|\tau\|^{k+2} |C(\tau)| < \infty$. We construct the estimator \widehat{M}_λ by replacing the unknown f and its derivatives in (19) with flat-top estimates producing

$$\widehat{M}_\lambda(\omega_1, \omega_2) = \left\{ \frac{\pi N}{\|\lambda\|_{L_2} \hat{f}(\omega_1) \hat{f}(\omega_2) \hat{f}(\omega_1 + \omega_2)} \left(\frac{\partial^2 \lambda(\tau_1, \tau_2)}{\partial \tau_1 \partial \tau_1} \Big|_{\tau_1 = \tau_2 = 0} \right)^2 \times \right. \\ \left. \times \left| \left(\frac{\partial^2}{\partial \omega_1^2} - \frac{\partial^2}{\partial \omega_1 \partial \omega_2} + \frac{\partial^2}{\partial \omega_2^2} \right) \hat{f}(\omega_1, \omega_2) \right|^2 \right\}^{\frac{1}{6}}$$

The next theorem provides convergence rates of the plug-in algorithm with flat-top pilots.

Theorem 3. Assume conditions on $\hat{\rho}$ such that (12) and (13) of Theorem 2 hold true, and assume conditions strong enough to ensure²

$$\text{var} \left(\widehat{f_{\omega_i, \omega_j}} \right) = O \left(\frac{M^{s-1}}{N} \right) \quad (i, j = 1, 2)$$

(i) Assume $C(\boldsymbol{\tau}) \sim A \|\boldsymbol{\tau}\|^{-d}$ for some positive constants A and $d > s + 2$. Then

$$\widehat{M}_\lambda = M_\lambda \left(1 + O_p \left(\left(\frac{\log N}{N} \right)^{\frac{[d-s-2]}{2d}} \right) \right).$$

(ii) Assume $C(\boldsymbol{\tau}) \sim A \xi^{\|\boldsymbol{\tau}\|}$ for some positive constant A and $|\xi| < 1$. Then

$$\widehat{M}_\lambda = M_\lambda \left(1 + O_p \left(\left(\frac{\log N}{N} \right)^{\frac{1}{2}} \right) \right).$$

(iii) Suppose $C(\boldsymbol{\tau}) = 0$ when $\|\boldsymbol{\tau}\| > q$, but $C(\boldsymbol{\tau}) \neq 0$ for some $\boldsymbol{\tau}$ with norm q , then

$$\widehat{M}_\lambda = M_\lambda \left(1 + O_p \left(\frac{1}{\sqrt{N}} \right) \right).$$

In many cases, the convergence is a significant improvement over the traditional plug-in approach with second-order lag-window pilots. For example, the convergence of the bandwidth for data from an ARMA process would be $M(1 + O_P(N^{-2/9}))$ using second-order pilots and techniques similar to [3, 4], but by using flat-top pilots, the convergence improves to $M(1 + O_P(\sqrt{\log N/N}))$.

5 Bispectral Simulations

The three lag-windows detailed above— λ_{opt} , λ_{rpf} , and λ_{rcf} —are compared by their mean square error performance in estimating the bispectrum of four standard time series models. Three criteria are used to evaluate the performance of the bispectral estimates. The first two criteria are the estimators performance in estimating the bispectrum at the two points $(0, 0)$ and $(2, 1)$. The bispectrum at the point $(0, 0)$ is real-valued, and estimates typically have variances significantly larger than estimates at the interior point $(2, 1)$ (exactly 30-times larger, asymptotically, if the second-order spectrum is flat). The bispectrum at the point $(2, 1)$ is complex valued and performance is evaluated based on the estimation of the real part, complex part, and absolute value. The third criteria of evaluation is a composite evaluation of performance of the estimators over a rough grid of six points, standardized appropriately (further details below). The simulations are computed with data from the four stationary time series models: iid χ_1^2 , ARMA(1,1), GARCH(1,1), and bilinear(1,0,1,1). The first two are linear time series models whereas the last two nonlinear models. Two sample sizes, $N = 200$ and $N = 2000$, are used throughout. Every simulation is repeated over 500 realizations.

²Certain mixing condition assumptions guarantee this; see [12] for an example.

The third criteria of evaluation, the composite evaluation is now described in further detail. The symmetries of C as given in (14) induce the following symmetries in the spectral density:

$$f(\omega_1, \omega_2) = f(\omega_2, \omega_1) = f(\omega_1, -\omega_1 - \omega_2) = f(-\omega_1 - \omega_2, \omega_2) = f^*(-\omega_1, -\omega_2)$$

The above symmetries in combination with the periodicity of f imply that f can be determined over the entire plane just by its values in the closed triangle T with vertices $(0, 0)$, $(\pi, 0)$, and $(2\pi/3, 2\pi/3)$. So f is estimated at $\binom{n-1}{2} = \frac{(n-1)(n-2)}{2}$ equally spaced points inside T with coordinates $\omega_{ij} = \left(\frac{\pi(2i+2j)}{3n}, \frac{2\pi j}{3n}\right)$ where $i = 1, \dots, n-1$ and $j = 1, \dots, n-i-1$ (we take $n = 5$ in the simulations).

The estimates at ω_{ij} are standardized to make them comparable. Since, for (ω_1, ω_2) inside T , [16]

$$\text{var} \left(\hat{f}(\omega_1, \omega_2) \right) \approx \frac{M^2}{N} \frac{\|\lambda\|_{L_2}}{2\pi} f(\omega_1) f(\omega_2) f(\omega_1 + \omega_2),$$

$\hat{f}(\omega_1, \omega_2)$ is standardized by dividing it by $\sqrt{f(\omega_1) f(\omega_2) f(\omega_1 + \omega_2)}$. This leads to the composite evaluation of \hat{f} over a coarse grid of points by the quantity

$$\text{err}(\lambda) \triangleq \sum_{i=1}^{n-1} \sum_{j=1}^{n-i-1} \left| \frac{\hat{f}(\omega_{ij}) - f(\omega_{ij})}{\sqrt{f(\omega_{ij}^{(1)}) f(\omega_{ij}^{(2)}) f(\omega_{ij}^{(1)} + \omega_{ij}^{(2)})}} \right|$$

and the empirical MSE is calculated by averaging $\text{err}(\lambda)^2$ over the 500 realizations.

In the tables of MSE estimates below, the first two rows are estimates from the flat-top lag-windows λ_{rpf} and λ_{rcf} with the bandwidth derived from the Bandwidth Selection Algorithm for the Bispectrum, as described above, with parameters $L = 5$, $c = .51$, and k determined via the block bootstrap (see Remarks 6 and 8). The third and fourth rows are estimates using the λ_{opt} with bandwidths from the plug-in method with flat-top pilots (f.p.) and second-order pilots (s.p.) respectively. The first column of each table concerns the estimation of the bispectrum at $(0, 0)$, taking absolute values if the estimate is complex valued. The next three columns concern the estimation of the real part, complex part, and absolute value of the bispectrum, respectively, at the point $(2, 1)$. The last column, labeled T_6 , concerns the composite evaluation over a coarse grid of 6 points.

Simulations (based on 1000 realizations) were conducted to determine the optimal finite-sample bandwidth with minimal MSE (checking up to a bandwidth size of 20). In the first three models—IID, ARMA, and GARCH—the optimal bandwidth is 1 under each evaluation criterion and every lag-window. The estimators with best MSE performance in these models were the estimators with the best bandwidth selection procedure (the choice of lag-window was somewhat secondary). The bilinear model, however, had different optimal bandwidths depending on the evaluation criterion and the lag-window. The optimal bandwidths for the bilinear model were incorporated into MSE tables by subscripting each value with the best bandwidth followed by the second best bandwidth. The optimality of the flat-top lag-window, independent of the bandwidth selection procedure, can be observed in this model as the optimal bandwidths are larger than 1.

Simulations are also carried out to study the bandwidth selection procedure for the bispectrum. Histograms, placed in Appendix B, depict the selected bandwidths for each model over 500 realizations under five procedures (a)–(e) described below. Procedure (a) produces bandwidths for flat-top lag-windows λ_{rpf} and λ_{rcf} whereas procedures (b) through (e) produce bandwidths for λ_{opt} .

- (a) Practical bandwidth selection algorithm for the bispectrum of Section 4
- (b) Plug-in method at the origin with flat-top pilots ³
- (c) Plug-in method at the point (2,1) with flat-top pilots³
- (d) Plug-in method at the origin with second-order pilots ⁴
- (e) Plug-in method at the point (2,1) with second-order pilots⁴

The performance of the above bandwidth selections procedures are evaluated by computing MSE estimates based on the simulations determining the optimal bandwidth. Since procedure (a) produces a global bandwidth, comparison is not so straightforward in the bilinear case where the optimal bandwidth at the origin is different from that of the interior.

5.1 IID Data

Identical and independent χ_1^2 data is generated with a central third moment $\mu_3 = 8$. Therefore the true bispectrum is $f(\omega_1, \omega_2) \equiv \frac{\mu_3}{(2\pi)^2} \approx .202642$. The following tables give the empirical MSE calculations of the estimated bispectrum over lengths $N = 200$ and $N = 2000$ based on 500 simulations.

$N = 200$	$ \hat{f}(0, 0) $	$\text{Re}\hat{f}(2, 1)$	$\text{Im}\hat{f}(2, 1)$	$ \hat{f}(2, 1) $	T_6
λ_{rpf}	0.02796	0.02061	3.131e-04	0.02093	709.4
λ_{rcf}	0.02778	0.02060	3.314e-04	0.02094	709.4
λ_{opt} (f.p.)	0.02582	0.02086	3.577e-04	0.02122	709.8
λ_{opt} (s.p.)	0.02806	0.02116	7.121e-04	0.02187	715.5
$N = 2000$	$ \hat{f}(0, 0) $	$\text{Re}\hat{f}(2, 1)$	$\text{Im}\hat{f}(2, 1)$	$ \hat{f}(2, 1) $	T_6
λ_{rpf}	2.887e-03	2.063e-03	1.799e-05	2.081e-03	71.19
λ_{rcf}	2.865e-03	2.064e-03	1.875e-05	2.083e-03	71.22
λ_{opt} (f.p.)	2.616e-03	2.101e-03	2.085e-05	2.121e-03	71.23
λ_{opt} (s.p.)	3.294e-03	2.184e-03	1.039e-04	2.288e-03	71.45

Table 1: MSE estimates based on iid data for $N = 200$ and $N = 2000$.

The flat-top estimators and λ_{opt} (f.p.) outperform λ_{opt} (f.p.) in every criterion considered. For $N = 2000$, bandwidth procedures (a), (b), and (c) perform extremely well

³The pilot estimates were derived from the flat-top lag-windows λ_{rpf} and the trapezoidal flat-top window [13]. The bandwidths for the pilot estimators are derived from the bandwidth selection algorithm of Section 3.

⁴The Parzen and optimal lag-windows were used as pilots with bandwidths $\lfloor N^{1/5} \rfloor$ and $\lfloor N^{1/6} \rfloor$ respectively.

(refer to the histograms in Figure 2 in Appendix B) producing the optimal bandwidth 1 over 95% of the time in each case.

5.2 ARMA Model

The ARMA(1,1) model

$$X_t = .5X_{t-1} - .5Z_{t-1} + Z_t$$

is now considered where $Z_t \stackrel{\text{iid}}{\sim} \mathcal{N}(0,1)$. This time series is Gaussian, so both the bispectrum and normalized bispectrum are identically zero.

$N = 200$	$ \hat{f}(0,0) $	$\text{Re}\hat{f}(2,1)$	$\text{Im}\hat{f}(2,1)$	$ \hat{f}(2,1) $	T_6
λ_{rpf}	6.102e-05	2.329e-05	4.468e-06	2.776e-05	313.3
λ_{rcf}	6.760e-05	2.435e-05	4.624e-06	2.897e-05	316.5
$\lambda_{\text{opt}}(\text{f.p.})$	4.422e-05	2.172e-05	5.235e-06	2.696e-05	302.8
$\lambda_{\text{opt}}(\text{s.p.})$	1.198e-04	3.088e-05	2.982e-05	6.070e-05	412.0
$N = 2000$	$ \hat{f}(0,0) $	$\text{Re}\hat{f}(2,1)$	$\text{Im}\hat{f}(2,1)$	$ \hat{f}(2,1) $	T_6
λ_{rpf}	2.997e-06	2.096e-06	6.896e-08	2.165e-06	24.21
λ_{rcf}	3.297e-06	2.137e-06	7.359e-08	2.210e-06	24.59
$\lambda_{\text{opt}}(\text{f.p.})$	3.129e-06	2.132e-06	2.796e-07	2.412e-06	24.74
$\lambda_{\text{opt}}(\text{s.p.})$	2.142e-05	4.222e-06	4.349e-06	8.571e-06	33.53

Table 2: MSE estimates based on arma data for $N = 200$ and $N = 2000$.

The flat-top estimators and $\lambda_{\text{opt}}(\text{f.p.})$ even more significantly outperform $\lambda_{\text{opt}}(\text{f.p.})$ in this model for every criterion considered. Good performance is mostly attributed to good bandwidth selection, but true optimal properties of the flat-top lag-windows is present and is addressed for the bilinear model.

5.3 GARCH Model

We now consider the GARCH(1,1) model

$$\begin{cases} X_t = \sqrt{h_t} Z_t \\ h_t = \alpha_0 + \alpha_1 X_{t-1}^2 + \alpha_2 h_{t-1} \end{cases}$$

where $\alpha = (.1, .8, .1)$ and $Z_t \stackrel{\text{iid}}{\sim} \mathcal{N}(0,1)$. The theoretical values of the bispectrum are unknown, so they are approximated via simulation over 500 realizations at a length of 10^5 and averaging the four estimators.

$N = 200$	$ \hat{f}(0,0) $	$\text{Re}\hat{f}(2,1)$	$\text{Im}\hat{f}(2,1)$	$ \hat{f}(2,1) $	T_6
λ_{rpf}	9.752e-04	5.462e-05	3.92e-05	9.383e-05	113.1
λ_{rcf}	1.038e-03	5.800e-05	4.391e-05	1.019e-04	115.1
$\lambda_{\text{opt}}(\text{f.p.})$	6.580e-04	4.345e-05	3.182e-05	7.527e-05	110.1
$\lambda_{\text{opt}}(\text{s.p.})$	3.849e-04	3.488e-05	5.112e-05	8.600e-05	125.1
$N = 2000$	$ \hat{f}(0,0) $	$\text{Re}\hat{f}(2,1)$	$\text{Im}\hat{f}(2,1)$	$ \hat{f}(2,1) $	T_6
λ_{rpf}	2.411e-05	2.916e-06	1.555e-06	4.471e-06	7.317
λ_{rcf}	2.682e-05	3.050e-06	1.745e-06	4.795e-06	7.401
$\lambda_{\text{opt}}(\text{f.p.})$	1.894e-05	2.528e-06	1.632e-06	4.159e-06	7.026
$\lambda_{\text{opt}}(\text{s.p.})$	5.781e-05	5.577e-06	7.577e-06	1.315e-05	9.021

Table 3: MSE estimates based on garch data for $N = 200$ and $N = 2000$.

For $N = 200$, $\lambda_{\text{opt}}(\text{s.p.})$ performed best at the origin, but considerably worse in the composite criterion. For the larger N , the flat-top estimators and $\lambda_{\text{opt}}(\text{f.p.})$ again performed significantly better than $\lambda_{\text{opt}}(\text{s.p.})$.

5.4 Bilinear Model

Finally, we consider the BL(1,0,1,1) bilinear model [16]

$$X_t = aX_{t-1} + bX_{t-1}Z_{t-1} + Z_t$$

where $a = b = .4$ and $Z_t \stackrel{\text{iid}}{\sim} \mathcal{N}(0,1)$. The complete calculations of the bispectrum have been worked out in [16], however the given equation for the bispectrum does not match-up with the simulations. Therefore theoretical values of the bispectrum were computed through simulations as done in the GARCH model. The spectral density equation provided in [16] is correct and was used.

Whereas the previous three models had an optimal bandwidth of 1 throughout, the optimal bandwidths for the bilinear model is typically much larger and depends on the evaluation criterion considered. The subscripted numbers represent the best and second best bandwidth for each window (as deduced from simulation).

$N = 200$	$ \hat{f}(0,0) $	$\text{Re}\hat{f}(2,1)$	$\text{Im}\hat{f}(2,1)$	$ \hat{f}(2,1) $	T_6
λ_{rpf}	5.872 _{2,3}	5.421e-04 _{4,5}	1.008e-03 _{1,2}	1.55e-03 _{4,5}	806.8 _{2,5}
λ_{rcf}	5.956 _{2,3}	6.005e-04 _{6,5}	1.073e-03 _{1,2}	1.673e-03 _{6,5}	817.0 _{7,6}
$\lambda_{\text{opt}}(\text{f.p.})$	4.401 _{2,1}	4.608e-04 _{4,3}	9.654e-04 _{1,2}	1.426e-03 _{4,3}	807.1 _{5,4}
$\lambda_{\text{opt}}(\text{s.p.})$	2.916 _{2,1}	3.926e-04 _{4,3}	8.623e-04 _{1,2}	1.255e-03 _{4,3}	791.4 _{5,4}
$N = 2000$	$ \hat{f}(0,0) $	$\text{Re}\hat{f}(2,1)$	$\text{Im}\hat{f}(2,1)$	$ \hat{f}(2,1) $	T_6
λ_{rpf}	1.755 _{4,3}	7.734e-05 _{4,6}	9.867e-05 _{1,2}	1.76e-04 _{4,6}	71.76 _{2,5}
λ_{rcf}	1.891 _{4,3}	7.792e-05 _{6,7}	1.012e-04 _{1,2}	1.791e-04 _{6,7}	74.69 _{6,7}
$\lambda_{\text{opt}}(\text{f.p.})$	2.119 _{4,3}	6.282e-05 _{5,6}	9.443e-05 _{1,2}	1.572e-04 _{5,4}	71.01 _{6,7}
$\lambda_{\text{opt}}(\text{s.p.})$	1.322 _{4,3}	5.123e-05 _{5,6}	8.064e-05 _{1,2}	1.319e-04 _{5,4}	72.83 _{6,7}

Table 4: MSE estimates based on bilinear data for $N = 200$ and $N = 2000$.

For this model, λ_{opt} (s.p.) performs better than the other three, but with decreasing margins with increased N . There is significant improvement of the flat-top estimators and λ_{opt} (f.p.) from $N = 200$ to $N = 2000$ making all the estimators mostly equivalent. The particularly good performance of λ_{opt} (s.p.) at the origin is due to a fortuitous bandwidth selection under sensitive conditions; this is addressed in more detail below.

There is somewhat of a discontinuity in optimal bandwidths for λ_{rpf} under the composite criterion as it jumps from a best value of 2 to a second best value of 5. A closer look at the MSEs for each bandwidth from 1 to 8 further illustrates this.

$N = 200$	1	2	3	4	5	6	7	8
λ_{rpf}	10200	331	851	442	423	457	440	454
λ_{rcf}	10200	471	985	561	458	457	454	464
λ_{opt}	6000	730	459	422	418	426	438	454

Table 5: MSE estimates of T_6 with bandwidths one through ten and $N = 200$

We see that the bandwidth 2 is very good for the flat-top lag-windows but very poor for λ_{opt} . Moreover, bandwidths 1 and 3 are extremely bad for the flat-top lag-window, and any bandwidth larger than 3 is mostly equivalent among the estimators. In the bandwidth selection procedure only odd integer bandwidths were selected since the last step of the procedure generates the bandwidth from dividing an integer by $b = c = .51$. If instead the parameter $c = .5$ is used, then only even integer bandwidths would be produced by the algorithm.

The bispectrum corresponding to bilinear model resembles a hill peaking at the origin [16]. This causes the choice of bandwidth to be particularly delicate when estimating the origin. The following table depicts this delicacy.

$N = 200$	1	2	3	4	5	6	7
λ_{rpf}	2.062	1.389	1.71	2.879	4.216	5.849	7.22
λ_{rcf}	2.062	1.390	1.864	3.207	4.848	6.502	8.078
λ_{opt}	1.823	1.445	2.013	3.13	4.448	5.733	6.852

Table 6: MSE estimates at the origin with bandwidths one through seven and $N = 200$

We see that selecting any bandwidth besides 2, or possibly 3, leads to a much larger mean square error. The bispectrum, however, is much flatter at points away from the origin, like the six interior points used in the composite evaluation. This causes the bandwidth to be less sensitive to the choice of bandwidth when estimating an interior value as seen in Table 5 above.

The simulations up to this point mostly depict the strength of the bandwidth selection procedure, and not the general asymptotic optimality of the flat-top lag-window. However, if we consider MSE estimates for a fixed set of bandwidths, as in Table 6, the flat-top estimates perform better than λ_{opt} which improves with N . The following table demonstrates the increased performance at $N = 2000$.

$N = 2000$	1	2	3	4	5	6	7	8
λ_{rpf}	2.029	0.9465	0.552	0.4687	0.6002	0.8262	1.029	1.237
λ_{rcf}	2.029	0.9082	0.5074	0.4917	0.6821	0.9224	1.156	1.346
λ_{opt}	1.736	0.8919	0.5444	0.5267	0.6444	0.8001	0.9579	1.099

Table 7: MSE estimates at the origin with bandwidths one through seven and $N = 200$

Further illustration of the optimality of the flat-top lag-windows is provided in [13] where second-order spectral density estimation with flat-top lag-windows is addressed.

5.5 Analysis of Bandwidth Procedures

Histograms of the bandwidths produced by the procedures are provided below. A summary of their performance is tabulated in the following table.

N	IID		ARMA		GARCH		Bilinear ^a	
	200	2000	200	2000	200	2000	200	2000
(a)	3.18	0.792	1.54	0.248	6.36	0.968	0.413	0.182
(b)	0.862	0.276	0.232	.050	2.59	0.292	1.63	0.454
(c)	2.71	0.900	0.866	0.142	4.05	0.552	0.633	0.362
(d)	1.45	3.96	1.27	3.22	1.19	3.49	0.185	0.414
(e)	4.66	12.0	4.04	9.36	4.22	9.82	0.0706	0.0394

^a Bandwidths 5 and 6 were selected as theoretical bandwidths for procedure (a), but this is only approximate as the optimal bandwidth varies. True theoretical bandwidths can be inferred from Table 4.

Table 8: MSE of $\hat{M}/M - 1$ for bandwidth selection procedures (a)–(e)

We see that the simple bandwidth selection algorithm is very effective in producing accurate bandwidths that are consistent. The bandwidth selection procedure (a) can be seen to be quite accurate from the histograms but tends to produce a few relatively large bandwidths. This error is compounded when squared error loss is used to evaluate the performance. The plug-in method with second-order pilots on the other hand performs very poorly and does not even appear consistent.

Histograms of the five bandwidth selection procedures are provided in Appendix B. The histograms in the first three models show a clear convergence of procedures (a) through (c) to the ideal bandwidth 1, whereas the bandwidths from procedures (d) and (e) grow with N . The histograms for the bilinear model show a general increase in M with N across each procedure.

6 Conclusions

Flat-top kernels in higher-order spectral density estimation is shown to be asymptotically superior in terms of MSE to any other finite-order kernel estimators. In addition, a very simple bandwidth selection algorithm is included that delivers ideal bandwidths tailored to the flat-top estimators. If one chooses not to adopt the infinite-order flat-top lag-window, then bandwidth selection via the plug-in method with flat-top pilots demonstrates greatly increased performance and should be used. Finite-sample simulations show these flat-top estimators were comparable with, and in many cases outperforming, the popular second-order “optimal” lag-window estimator using the plug-in method with second-order pilots for bandwidth selection. Simulations show the estimation of the bispectrum is quite sensitive to the choice of bandwidth, and this paper delivers the first higher-order accurate bandwidth selection procedures for the bispectrum.

A Technical proofs

Lemma 1. *The expectation of $\widehat{C}(\boldsymbol{\tau})$ is*

$$\mathbb{E} \left[\widehat{C}(\boldsymbol{\tau}) \right] = \left(1 - \frac{\gamma}{N} \right) C(\boldsymbol{\tau}) + O \left(\frac{1}{N} \right).$$

PROOF OF LEMMA 1. Let $\mathbf{y}_t = \mathbf{x}_t - \boldsymbol{\mu}$, then

$$\begin{aligned} \mathbb{E} \left[\widehat{C}(\boldsymbol{\tau}) \right] &= \frac{1}{N} \sum_{t=1}^{N-\gamma} \mathbb{E} \left[\prod_{j=1}^s (x_{t-\alpha+\tau_j}^{(a_j)} - \bar{x}^{(a_j)}) \right] \\ &= \frac{1}{N} \sum_{t=1}^{N-\gamma} \mathbb{E} \left[\prod_{j=1}^s \left((x_{t-\alpha+\tau_j}^{(a_j)} - \mu^{(a_j)}) + (\mu^{(a_j)} - \bar{x}^{(a_j)}) \right) \right] \\ &= \frac{1}{N} \sum_{t=1}^{N-\gamma} \mathbb{E} \left[\prod_{j=1}^s (y_{t-\alpha+\tau_j}^{(a_j)} - \bar{y}^{(a_j)}) \right] \\ &= \frac{1}{N} \sum_{t=1}^{N-\gamma} C(\boldsymbol{\tau}) + \sum_{\boldsymbol{\delta} \in \mathcal{V}} \mathbb{E} \left[\prod_{j=1}^s \left(y_{t-\alpha+\tau_j}^{(a_j)} \right)^{1-\delta_j} \left(\bar{y}^{(a_j)} \right)^{\delta_j} \right]. \end{aligned}$$

In the summation above, \mathcal{V} denotes the set of all binary s -tuples excluding the s -tuple $\{0, \dots, 0\}$; \mathcal{V} has cardinality $2^s - 1$. Let $\boldsymbol{\delta} \in \mathcal{V}$ and ℓ be its weight, i.e. $\ell = \sum_{j=1}^s \delta_j$. Let us suppose, w.l.o.g., that the first ℓ components of $\boldsymbol{\delta}$ are 1 and the rest 0. Then

the term in the above summation corresponding to this δ can be written as

$$\begin{aligned}
\mathbb{E} \left[\prod_{j=1}^{\ell} \bar{y}^{(a_j)} \prod_{j=\ell+1}^s y_{t-\alpha+\tau_j}^{(a_j)} \right] &= \frac{1}{N^\ell} \sum_{u_1=1}^N \cdots \sum_{u_\ell=1}^N \mathbb{E} \left[\prod_{i=1}^{\ell} y_{u_i}^{(a_i)} \prod_{j=\ell+1}^s y_{t-\alpha+\tau_j}^{(a_j)} \right] \\
&= \frac{1}{N^\ell} \sum_{u_1=1}^N \cdots \sum_{u_\ell=1}^N C(u_1, \dots, u_\ell, t - \alpha + \tau_{\ell+1}, \dots, t - \alpha + \tau_s) \\
&= O\left(\frac{1}{N}\right).
\end{aligned}$$

The last equality follows from the absolute summability of $C(\boldsymbol{\tau})$. Since for every $\delta \in \mathcal{V}$ the expectation as above is $O(N^{-1})$, the result follows.

PROOF OF THEOREM 1. Using Lemma 1 and property (iii) of the lag-window, the expectation of $\hat{f}(\boldsymbol{\omega})$ can be expressed as

$$\begin{aligned}
E[\hat{f}(\boldsymbol{\omega})] &= \frac{1}{(2\pi)^{s-1}} \sum_{\|\boldsymbol{\tau}\| < N} \left(\left(1 - \frac{\gamma}{N}\right) C(\boldsymbol{\tau}) + O\left(\frac{1}{N}\right) \right) \lambda_M(\boldsymbol{\tau}) e^{-i\boldsymbol{\tau} \cdot \boldsymbol{\omega}} \\
&= \frac{1}{(2\pi)^{s-1}} \sum_{\|\boldsymbol{\tau}\| < N} \left(1 - \frac{\gamma}{N}\right) C(\boldsymbol{\tau}) \lambda_M(\boldsymbol{\tau}) e^{-i\boldsymbol{\tau} \cdot \boldsymbol{\omega}} + O\left(\frac{M^{s-1}}{N}\right).
\end{aligned}$$

The bias of $\hat{f}(\boldsymbol{\omega})$ is

$$\begin{aligned}
E[\hat{f}(\boldsymbol{\omega})] - f(\boldsymbol{\omega}) &= \frac{1}{(2\pi)^{s-1}} \sum_{\|\boldsymbol{\tau}\| < N} \left(\lambda_M(\boldsymbol{\tau}) \left(1 - \frac{\gamma}{N}\right) - 1 \right) C(\boldsymbol{\tau}) e^{-i\boldsymbol{\tau} \cdot \boldsymbol{\omega}} \\
&\quad - \frac{1}{(2\pi)^{s-1}} \sum_{\|\boldsymbol{\tau}\| \geq N} C(\boldsymbol{\tau}) e^{-i\boldsymbol{\tau} \cdot \boldsymbol{\omega}} + O\left(\frac{M^{s-1}}{N}\right) \\
&= \underbrace{\frac{1}{(2\pi)^{s-1}} \sum_{\|\boldsymbol{\tau}\| < N} (\lambda_M(\boldsymbol{\tau}) - 1) C(\boldsymbol{\tau}) e^{-i\boldsymbol{\tau} \cdot \boldsymbol{\omega}}}_{A_1} \\
&\quad - \underbrace{\frac{1}{(2\pi)^{s-1} N} \sum_{\|\boldsymbol{\tau}\| < N} \gamma \lambda_M(\boldsymbol{\tau}) C(\boldsymbol{\tau}) e^{-i\boldsymbol{\tau} \cdot \boldsymbol{\omega}}}_{A_2} \\
&\quad - \underbrace{\frac{1}{(2\pi)^{s-1}} \sum_{\|\boldsymbol{\tau}\| \geq N} C(\boldsymbol{\tau}) e^{-i\boldsymbol{\tau} \cdot \boldsymbol{\omega}} + O\left(\frac{M^{s-1}}{N}\right)}_{A_3}
\end{aligned}$$

By the assumption on the summability of $C(\boldsymbol{\tau})$, $|A_3|$ can be bounded as

$$|A_3| \leq \frac{1}{(2\pi)^{s-1}} \sum_{\|\boldsymbol{\tau}\| \geq N} |C(\boldsymbol{\tau})| \leq \frac{1}{(2\pi)^{s-1} N^k} \sum_{\|\boldsymbol{\tau}\| \geq N} \|\boldsymbol{\tau}\|^k |C(\boldsymbol{\tau})| = o\left(\frac{1}{N^k}\right)$$

Also,

$$|A_2| \leq \frac{1}{(2\pi)^{s-1}N} \sum_{\|\boldsymbol{\tau}\| < N} |\gamma| |C(\boldsymbol{\tau})| = O\left(\frac{1}{N}\right)$$

Now rewrite A_1 as

$$A_1 = \underbrace{\frac{1}{(2\pi)^{s-1}} \sum_{\|\boldsymbol{\tau}\| \leq bM} (\lambda_M(\boldsymbol{\tau}) - 1) C(\boldsymbol{\tau}) e^{-i\boldsymbol{\tau} \cdot \boldsymbol{\omega}}}_{=0} + \frac{1}{(2\pi)^{s-1}} \sum_{bM < \|\boldsymbol{\tau}\| \leq N} (\lambda_M(\boldsymbol{\tau}) - 1) C(\boldsymbol{\tau}) e^{-i\boldsymbol{\tau} \cdot \boldsymbol{\omega}}$$

PROOF OF (i).

Since $|\lambda(\mathbf{s})| \leq 1$,

$$|A_1| \leq \frac{2}{(2\pi)^{s-1}} \sum_{bM < \|\boldsymbol{\tau}\| \leq N} |C(\boldsymbol{\tau})| \leq \frac{2}{(2\pi)^{s-1}(bM)^k} \sum_{bM < \|\boldsymbol{\tau}\| \leq N} \|\boldsymbol{\tau}\|^k |C(\boldsymbol{\tau})| = o\left(\frac{1}{M^k}\right)$$

Equation (6) now follows, and thus $\text{MSE}(\hat{f}(\boldsymbol{\omega})) \sim o(M^{-2k}) + O(M^{s-1}/N)$.

PROOF OF (ii).

We have $\text{bias}(\hat{f}(\boldsymbol{\omega})) = A_1 + O(M^{s-1}/N)$, where under the assumptions of (ii),

$$|A_1| \leq \frac{2}{(2\pi)^{s-1}} \sum_{bM < \|\boldsymbol{\tau}\| \leq N} |C(\boldsymbol{\tau})| \leq \frac{(2)D}{(2\pi)^{s-1}e^{dbM}} \sum_{bM < \|\boldsymbol{\tau}\| \leq N} e^{d(bM - \|\boldsymbol{\tau}\|)} = O\left(e^{-dbM}\right).$$

Therefore $\text{MSE}(\hat{f}(\boldsymbol{\omega})) \sim O(e^{-2dbM}) + O(M^{s-1}/N)$ is asymptotically minimized when $M \sim A \log N$ where $A = 1/(2db)$, and (8) holds for all $A \geq 1/(2db)$.

PROOF OF (iii).

We have $\text{bias}(\hat{f}(\boldsymbol{\omega})) = A_1 + O(M^{s-1}/N)$, but under the assumptions of (iii), $A_1 = 0$. Hence the bias and variance are $O(1/N)$.

PROOF OF THEOREM 2. Let $\boldsymbol{\tau}_{\hat{m}}$ be any element of norm \hat{m} for which

$$|\hat{\rho}(\boldsymbol{\tau}_{\hat{m}})| > k \sqrt{\frac{\log N}{N}} \quad (21)$$

and let $\boldsymbol{\tau}'_{\hat{m}} \in B_{\hat{m}, \hat{m}+1}$, so that $\hat{m} < \|\boldsymbol{\tau}'_{\hat{m}}\| \leq \hat{m} + 1$, and

$$|\hat{\rho}(\boldsymbol{\tau}'_{\hat{m}})| < k \sqrt{\frac{\log N}{N}} \quad (22)$$

Equations (10) and (13) give

$$|\hat{\rho}(\boldsymbol{\tau}_{\hat{m}})| = |\rho(\boldsymbol{\tau}_{\hat{m}})| + o_p\left(\sqrt{\frac{\log \log N}{N}}\right) \quad (23)$$

In part (i), $\rho(\boldsymbol{\tau}) \sim A\|\boldsymbol{\tau}\|^{-d}$, so for any $\epsilon > 0$, we can find τ_0 such that

$$A(1 - \epsilon)\|\boldsymbol{\tau}\|^{-d} < \rho(\boldsymbol{\tau}) < A(1 + \epsilon)\|\boldsymbol{\tau}\|^{-d} \quad (24)$$

when $\|\boldsymbol{\tau}\| > \tau_0$. Similarly, for any $\epsilon > 0$, there exists τ_0 large enough such that

$$(1 - \epsilon)\hat{m}^{-d} < \|\boldsymbol{\tau}\|^{-d} < (1 + \epsilon)\hat{m}^{-d} \quad \text{for all } \boldsymbol{\tau} \in B_{\hat{m}, \hat{m}+1} \quad (25)$$

when $\hat{m} > \tau_0$. Putting equations (21), (22), (23), (24), and (25) together gives, with high probability,

$$A(1 - \epsilon)^2\hat{m}^{-d} < c\sqrt{\frac{\log N}{N}} < A(1 + \epsilon)^2\hat{m}^{-d} \quad (26)$$

up to $o_p(\sqrt{(\log \log N)/N})$, which is negligible as N gets large. Equation (26) is equivalent to

$$\frac{\hat{m}}{(1 + \epsilon)^2} < \frac{A^{1/d}N^{1/2d}}{k^{1/d}(\log N)^{1/2d}} < \frac{\hat{m}}{(1 - \epsilon)^2}$$

with high probability. Therefore

$$\hat{m} \stackrel{P}{\sim} \frac{A^{1/d}N^{1/2d}}{k^{1/d}(\log N)^{1/2d}}$$

The proof of part (ii) is similar.

Now we prove part (iii). Note that $\hat{m} > q$ only if

$$\max_{\boldsymbol{\tau} \in B_{q, q+a_N}} |\hat{\rho}(\boldsymbol{\tau}) - \rho(\boldsymbol{\tau})| \geq k\sqrt{\frac{\log N}{N}} \quad (27)$$

but since $C(\boldsymbol{\tau}) = 0$ when $\|\boldsymbol{\tau}\| > q$, equation (13) then shows

$$\max_{\boldsymbol{\tau} \in B_{q, q+a_N}} |\hat{\rho}(\boldsymbol{\tau})| = o_p\left(\sqrt{\frac{\log \log N}{N}}\right) \quad (28)$$

since $a_N = o(\log N)$. The probability of (27) and (28) happening simultaneously tends to zero, hence $P(\hat{m} > q) \rightarrow 0$. Now if $\hat{m} < q$ then

$$B_{\hat{m}, \hat{m}+a_N} |\hat{\rho}(\boldsymbol{\tau})| = |\rho(\boldsymbol{\tau})| + o_p\left(\sqrt{\frac{\log \log N}{N}}\right)$$

shows that (10) must eventually be violated, hence $P(\hat{m} < q) \rightarrow 0$ and the result follows.

PROOF OF THEOREM 3. Parts (ii) and (iii) follow from Theorems 1 and 2 and the δ -method; see [12] for more details. For part (i), first note that $\sum_{\boldsymbol{\tau} \in \mathbb{Z}^{s-1} \setminus \{\mathbf{0}\}} \|\boldsymbol{\tau}\|^\alpha < \infty$ if and only if $\alpha > s - 1$. In order for $\sum_{\boldsymbol{\tau} \in \mathbb{Z}^{s-1}} \|\boldsymbol{\tau}\|^{k+2} |C(\boldsymbol{\tau})| < \infty$, for some $k \geq 1$, d must satisfy $d - k - 2 > s - 1$ or $d > s + k + 1 \geq s + 2$. Now the results of Theorem 1 hold for $\widehat{f_{\omega_i, \omega_j}}$ in replace of $\hat{f}(\omega_1, \omega_2)$ for any positive integer $k < d - s - 1$, in particular for $k = \lceil d - s - 2 \rceil$. From the proof of Theorem 1, the bias is of order $o(1/M^k)$, and since the variance is of smaller order, the result now follows from substituting M with the rate $(N/\log N)^{1/2d}$ from Theorem 2 (i).

B Histograms

Below are histograms of the bandwidth selection procedures (a) through (e) based on iid data. The top row in every Figure corresponds to $N = 200$ and the bottom row corresponds to $N = 2000$.

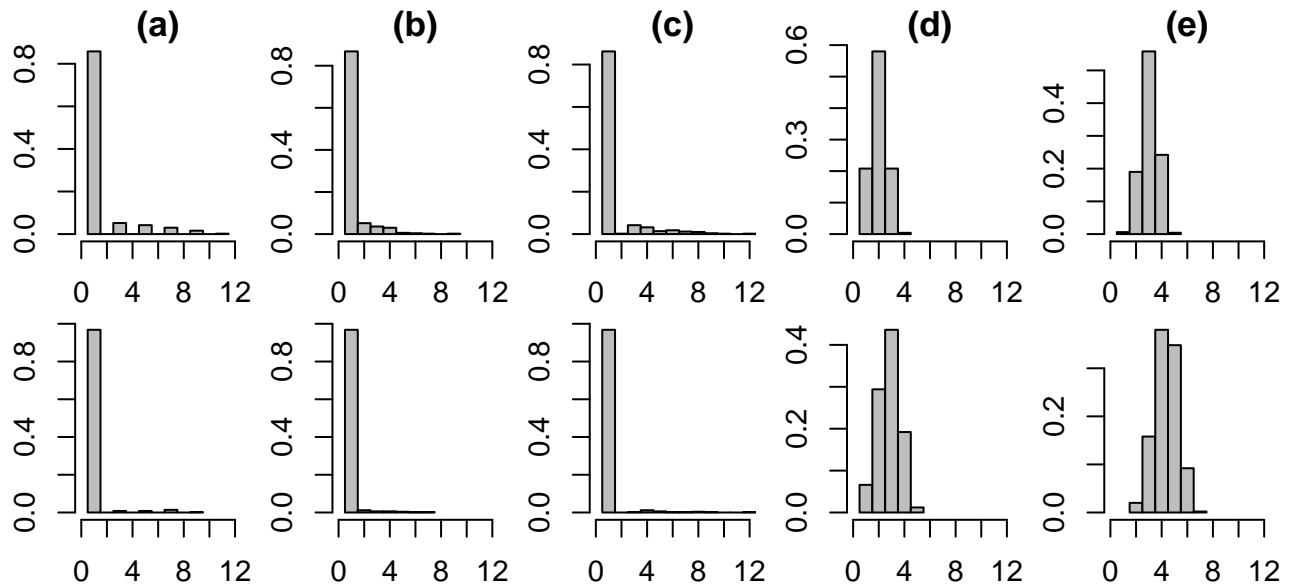


Figure 2: Histograms based on iid data.

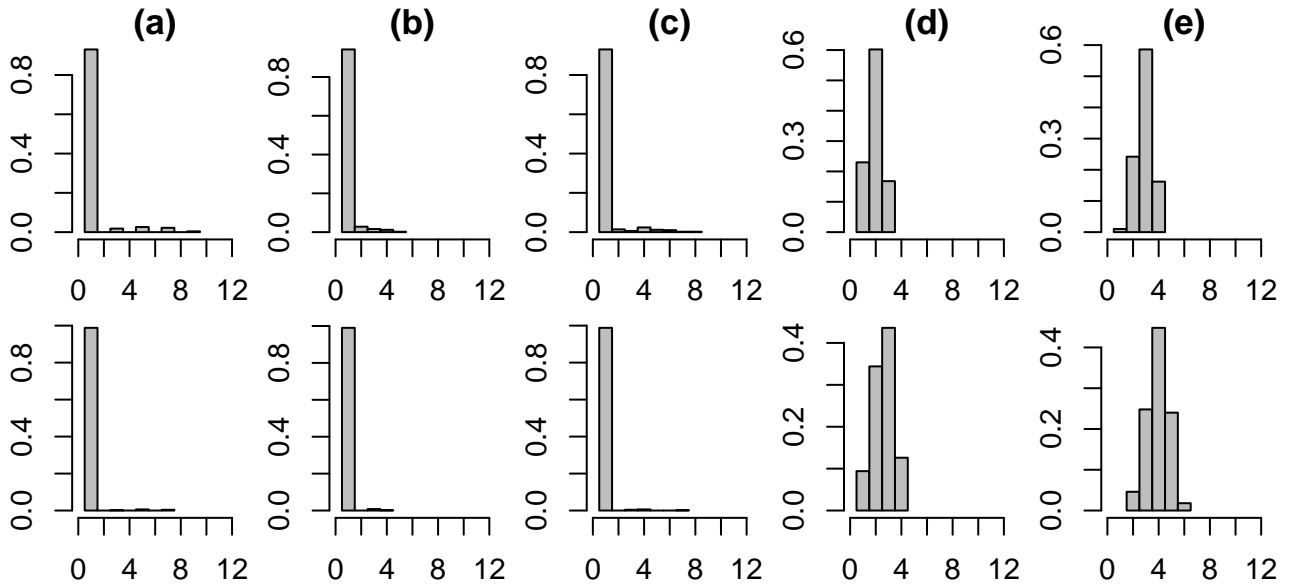


Figure 3: Histograms based on arma data.

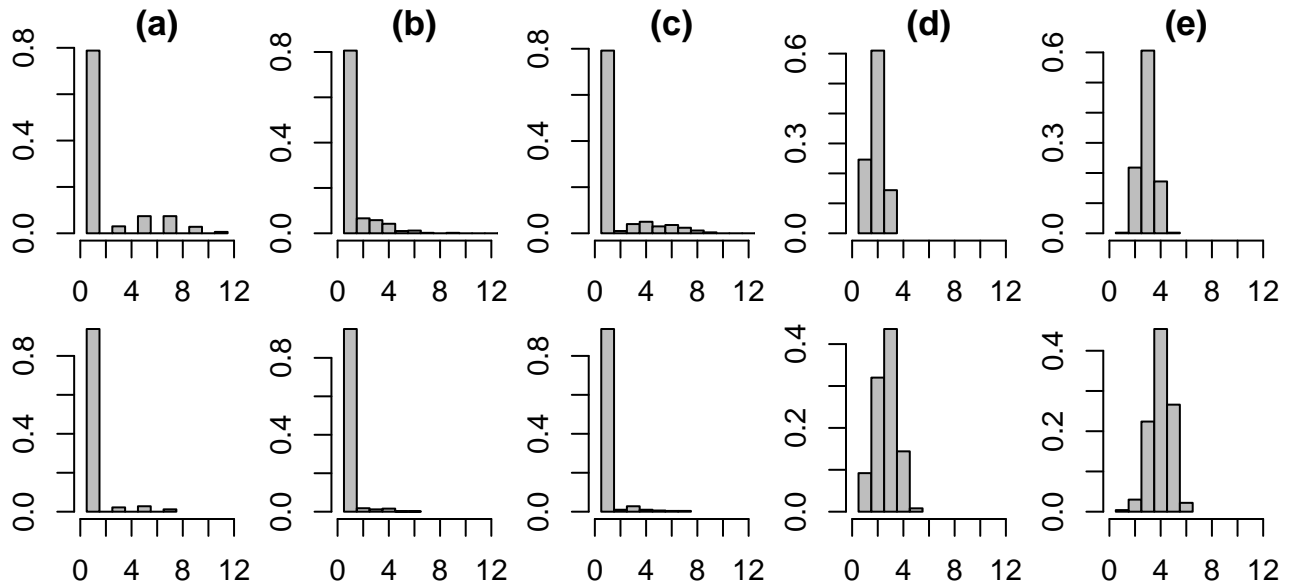


Figure 4: Histograms based on garch data.

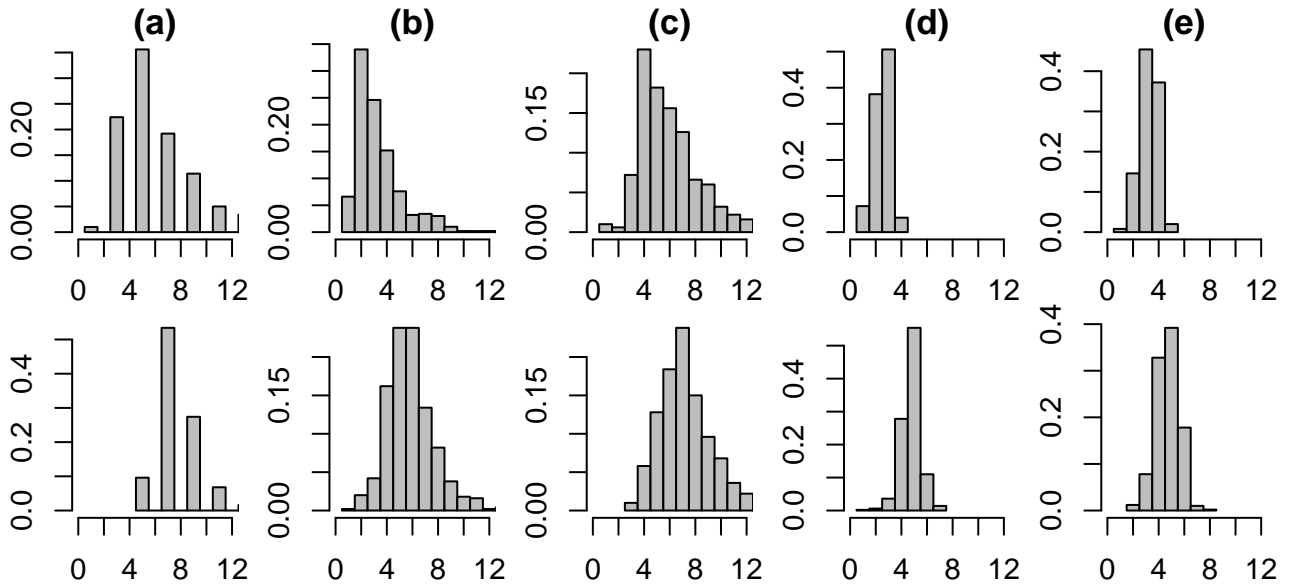


Figure 5: Histograms based on bilinear data.

References

- [1] David R. Brillinger and Murray Rosenblatt. Asymptotic theory of estimates of k -th order spectra. In *Spectral Analysis Time Series (Proc. Advanced Sem., Madison, Wis., 1966)*, pages 153–188. John Wiley, New York, 1967.
- [2] David R. Brillinger and Murray Rosenblatt. Computation and interpretation of k -th order spectra. In *Spectral Analysis Time Series (Proc. Advanced Sem., Madison, Wis., 1966)*, pages 189–232. John Wiley, New York, 1967.
- [3] Michael Brockmann, Theo Gasser, and Eva Herrmann. Locally adaptive bandwidth choice for kernel regression estimators. *J. Amer. Statist. Assoc.*, 88(424): 1302–1309, 1993. ISSN 0162-1459.
- [4] Peter Bühlmann. Locally adaptive lag-window spectral estimation. *J. Time Ser. Anal.*, 17(3):247–270, 1996. ISSN 0143-9782.
- [5] Peter Hall and J. S. Marron. Choice of kernel order in density estimation. *Ann. Statist.*, 16(1):161–173, 1988. ISSN 0090-5364.
- [6] Melvin J. Hinich. Testing for Gaussianity and linearity of a stationary time series. *J. Time Ser. Anal.*, 3(3):169–176, 1982. ISSN 0143-9782.

- [7] S.R. Jammalamadak, T.S. Rao, and György Terdik. Higher order cumulants of random vectors and applications to statistical inference and time series. *Sankhyā*, 68(2):326–356, 2006.
- [8] M. C. Jones, J. S. Marron, and S. J. Sheather. A brief survey of bandwidth selection for density estimation. *J. Amer. Statist. Assoc.*, 91(433):401–407, 1996. ISSN 0162-1459.
- [9] M. R. Leadbetter, Georg Lindgren, and Holger Rootzén. *Extremes and related properties of random sequences and processes*. Springer Series in Statistics. Springer-Verlag, New York, 1983. ISBN 0-387-90731-9.
- [10] K. S. Lii and M. Rosenblatt. Cumulant spectral estimates: bias and covariance. In *Limit theorems in probability and statistics (Pécs, 1989)*, volume 57 of *Colloq. Math. Soc. János Bolyai*, pages 365–405. North-Holland, Amsterdam, 1990.
- [11] K. S. Lii and M. Rosenblatt. Asymptotic normality of cumulant spectral estimates. *J. Theoret. Probab.*, 3(2):367–385, 1990. ISSN 0894-9840.
- [12] Dimitris N. Politis. Adaptive bandwidth choice. *J. Nonparametr. Stat.*, 15(4-5): 517–533, 2003. ISSN 1048-5252.
- [13] Dimitris N. Politis and Joseph P. Romano. Bias-corrected nonparametric spectral estimation. *J. Time Ser. Anal.*, 16(1):67–103, 1995. ISSN 0143-9782.
- [14] Keiichi Saito and Tomoharu Tanaka. Exact analytic expression for gabr-rao’s optimal bispectral two-dimensional lag window. *J. Nucl. Sci. Technol.*, 22(12): 1033–1035, 1985.
- [15] T. Subba Rao and M. M. Gabr. A test for linearity of stationary time series. *J. Time Ser. Anal.*, 1(2):145–158, 1980. ISSN 0143-9782.
- [16] T. Subba Rao and M. M. Gabr. *An introduction to bispectral analysis and bilinear time series models*, volume 24 of *Lecture Notes in Statistics*. Springer-Verlag, New York, 1984. ISBN 0-387-96039-2.
- [17] T. Subba Rao and Gy. Terdik. On the theory of discrete and continuous bilinear time series models. In *Stochastic processes: modelling and simulation*, volume 21 of *Handbook of Statist.*, pages 827–870. North-Holland, Amsterdam, 2003.